

# Dynamic behavior of horizontally curved multi-girder express highway bridge under moving vehicle

Hokkaido University  
Hokkaido University  
Hokkaido University  
Hokkaido University  
NEXCO Engineering Hokkaido  
Rajshahi University of Engineering & Technology

Student member ○ Md Basir ZISAN  
Fellow member Toshiro HAYASHIKAWA  
Member Takashi MATSUMOTO  
Member Xingwen HE  
Member Tetsuji OHTA  
Student member Md Robiul AWALL

## 1 Introduction

Horizontally curved bridges at highway interchange has gained much more popularity because of smooth dissemination of congested traffic, simplicity in arrangement, details and construction and limitation of right of way. Structural complexities of curve bridges inspiring the researchers to investigate the dynamic response characteristics of curve bridge. Prediction of bridges response resulting from moving vehicles is of significance in bridge design because a moving vehicle causes larger response on structure than static does. Present practice of bridge design is to multiply the static response using a numerical value called Impact Factor (IF) defined by AASHTO & JRA code to account for the effect of moving vehicles. Although both formulae defined Dynamic Amplification Factor (DAF) as a function of bridge span length, after investigation it is found that DAF depends on numerous bridge-vehicle parameters.

Sennah and Kennedy [1] studied horizontally curve box girder bridge assuming vehicle as a concentrated moving load and ignoring the surface roughness found that speed of vehicle have a significant influence on impact factor. Again Senthilvasan et. al. [2] and Sennah et. al. [3] found DAF value influenced by both position of vehicle along longitudinal and transverse direction. The most important finding is that torsional modes of vibration induced by curvature influence DAF significantly. The couple bending and torsion induced by horizontal curvature and little torsional stiffness of I-girder described by Linzell et. al. [4] emphasized the demand for evaluation of dynamic behavior of curve girder bridge and also curvature effect on DAF. Mermertas [5] described bridge curvature significantly increase the dynamic deflection. A numerical study carried by Huang et. al. [6] shows impact of curvature on shear and bending moment of multi-girder bridge and found curvature increase both torsion and bi-moment significantly. Here the relations of DAF with bridge curvatures remain unclear. All aforementioned works significantly improved bridge vehicle interaction problem with some limitation itself but DAFs for curve girder bridge influenced by bridge-vehicle parameters in reality remains vague.

The purpose of this study is to identify the effect of vehicle speed, loading position on traffic lane, road and bridge surface roughness, bridge curvature and bump height on DAF and also verifying the effectiveness of AASHTO and JRA specified formulae with obtain DAF value. A 3D FE model of multi-girder bridge and HS20-44 design truck has developed using ANSYS APDL. The procedure considered the inertia force, curvature effect,

deck friction, surface to node contact technology and also vehicle model includes the effect of pitching, rolling, bouncing and separation between tires and bridge surface.

## 2 Analytical Modeling

### 2.1 FE modeling of bridge

The real bridge considered in this study is Kita-go multi girder continuous bridge situated in Sapporo, Japan. The bridge has radius  $R=1000$  m and three spans about 50 m each. The five I-girders of different geometry are 2.8m deep and equally spaced by 2.1 m. These main structural members tied together with reinforced concrete slab which acts compositely with main girders and 10 equally spaced diaphragms. The basic geometric properties of Kita-go bridge is shown in **Table 1** and **Fig. 1**. A 3D FE model of studied bridge has developed using ANSYS APDL as shown in **Fig. 2**. The concrete deck and steel member are modeled by using 8-noded solid 45 hexagonal elements and 4-noded quadrilateral shell 63 elements respectively. Cylindrical coordinate system having origin at center of curvature of bridge has used to define all geometric properties of FE model. Simply supported boundary condition roller and hinge supports are applied at bottom flange node at each girder end. The roller support can move horizontally along tangential direction whereas horizontal displacement of hinged support has restrained. All supports are restrained in vertical direction but allow rotating along support line. The boundary conditions are shown in **Table 2**. A concrete having mass density  $2500 \text{ kg/m}^3$ , modulus of elasticity 28.57 GPa and Poisson ratio 0.20 has used for deck section and for all steel members, a mass density  $7850 \text{ kg/m}^3$ , modulus of elasticity 210 GPa and Poisson ratio 0.30 were used.

### 2.2 Bridge vehicle interaction modeling

A 3-D nonlinear FE model of HS20-44 design truck specified by AASHTO shown in **Fig. 3(a)** is developed using ANSYS as shown in **Fig. 3(b)** which consists of five lump masses with rotary inertia representing tractor, semi-trailer and three axle sets. All masses connected by rigid beams and supported by linear spring-damper are modeled by BEAM4 and MASS21 element and spring dampers are modeled by COMBIN40 element. Separation between wheel tires and road surface is integrated using gap element at lower spring-damper. The tires stiffness and spring suspension values as shown in **Table 3** are found from Wang et. al. [7]. To simulate the effect of road roughness, an actuator modeled by LINK11 is connected with gap element. CONTA 174 and TARGE 170 elements

Table 1: Structural geometric property of Kita-go bridge

Span length [mm]	49913			
Deck width*thickness [mm]	11000*20			
Web of main girder [mm]	WEB 2800*10			
Flange of main girder [mm]	FLGG1:540*25	FLGG2:350*16	FLGG3&4:370*14	FLGG5:510*25
Vertical Stiffener of main girder [mm]	145*12			
Horizontal Stiffener of main girder [mm]	115*11			
Flange and Web of Intermediate Diaphragm [mm]	IFLG 100*8 and IWEB 200*8			
Vertical Stiffener of Intermediate Diaphragm [mm]	145*12			
Flange and Web of End Diaphragm [mm]	EFLG 250*10 and EWEB 2400*9			
Vertical Stiffener of End Diaphragm [mm]	145*22			
Flange and Web of Lateral Bracing [mm]	LWEB 150*10 and LFLG 150*12			

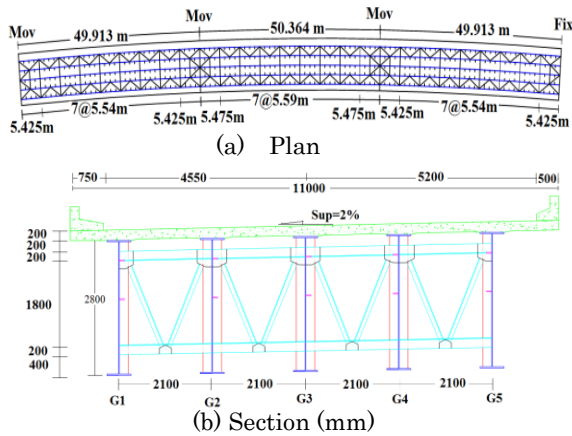


Fig. 1. Structural geometry of Kita-go

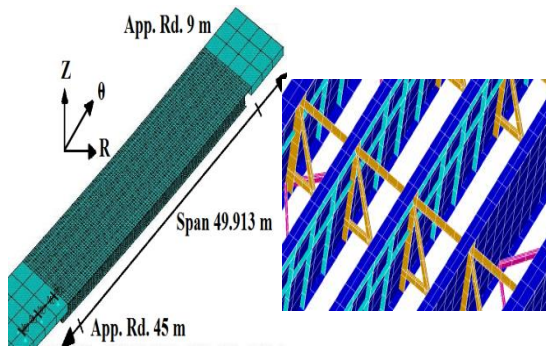
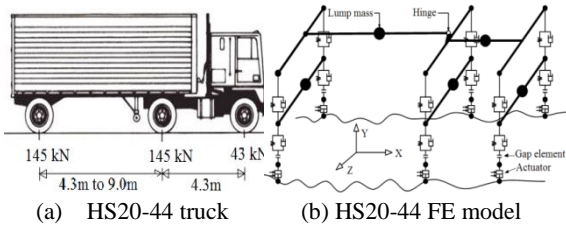


Fig. 2. FE model of of Kita-go bridge



(a) HS20-44 truck (b) HS20-44 FE model  
Fig. 3. HS20-44 design truck

are used to generate node to contact surface and target surface to establish dynamic interaction between bridge and tires, respectively. An isotropic coulomb friction of value 0.18 is assumed for all cases as defined by Samman et. al. [8]. This contact analysis dramatically adds non-linearity of the analysis. Newmark's  $\beta$  and Newton-Raphson methods with full transient analysis options are used to calculate structural response at each discrete time step.

### 3 Free Vibration and Model Validation

Natural vibration characteristics defined by mode shapes and natural frequencies of a structure indicates how it will respond under dynamic loadings. Since actual bridges has 2% super elevation, hence natural vibration analysis is performed both for 0% and 2% super elevation. From **Table 4**, it is found that mode shape and natural frequency has a good agreement with experimental results. So, the develop FE model of Kita-go bridge is applicable for dynamic analysis. The **Table 4** also shows that effect of super elevation on natural frequency is negligible because of large radius of curvature. It is also proved by Awall et. al. [9] that

Table 2: Boundary conditions

Support condition	$u_1$	$u_2$	$u_3$	$\theta_1$	$\theta_2$	$\theta_3$
Roller	Fix	Free	Fix	Free	Free	Free
Hinged	Fix	Fix	Fix	Free	Free	Free

$u_1, u_2, u_3$  are translations in  $R, \theta, Z$  directions  
 $\theta_1, \theta_2, \theta_3$  are rotations in  $R, \theta, Z$  directions

Table 3: Stiffness coefficient of HS20-44

	Front axle (kN/cm)	Drive axle (kN/cm)	Semi-trailer axle (kN/cm)
Tire	8.75	35.03	35.07
Suspension spring	2.43	19.03	16.69

Table 4: Natural frequency of Kita-go Bridge

Super Elevation	Mode 1	Mode 2	Mode 3	Mode 4	Mode 5
0%	2.29	4.02	6.70	7.97	10.39
2%	2.28	4.00	6.84	7.92	10.33
Experiment	2.50	--	--	7.14	--

Table 5: Natural frequency of AASHTO HS20-44 truck

Mode	Frequency (Hz)	Nature of mode
1 <sup>st</sup>	1.47	Rolling (2 <sup>nd</sup> rear axle)
2 <sup>nd</sup>	1.79	Pitching
3 <sup>rd</sup>	2.06	Bouncing (Front axle)
4 <sup>th</sup>	2.21	Bouncing
5 <sup>th</sup>	4.02	Rolling (Front & 1 <sup>st</sup> rear axle)

horizontally curved bridge having curvature more than 800 m has no super elevation effect on natural vibration. The natural vibration analysis result for first five modes of AASHTO HS20-44 truck is shown in **Table 5**.

### 4 Road Roughness Modeling

Bridge Dynamic response is significantly affected by approach road and bridge deck roughness conditions. Dodds et. al. [10] and Honda et. al. [11] assumed road surface roughness as periodically modulated random process derived from Power Spectral Density function using Eq.(1)

$$S(n) = S(n_0) \left(\frac{n}{n_0}\right)^{-w} \dots \dots \dots (1)$$

where  $S(n)$  = PSD ( $m^2/cycle/m$ );  $n$  = wave number ( $cycle/m$ );  $S(n_0)$  = roughness coefficient ( $m^2/cycle/m$ );  $n_0$  = discontinuity frequency =  $1/(2\pi)$ ; Based on Motor Industry Research Association specification [12], for principle road  $w = 2$  (1.36 ~2.28) and roughness coefficient  $20 \times 10^{-6}$  is used for good road surface. Awall et. al. [9] generated correlated road surface profile from PSD and cross spectral density functions considering road surface as a homogenous and isotropic random process using Eq.(2) proposed by Dodds et. al. [10]

$$y_R(x) = \sum_{i=1}^N \left( \frac{\sqrt{\Delta n_i} \cdot S_x(n_i) \cdot \cos(2\pi n_i x + \phi_i) + \dots}{\sqrt{\Delta n_i} (S(n_i) - S_x(n_i)) \cdot \cos(2\pi n_i x + \theta_i)} \right) \dots \dots (2)$$

Where  $S_x(n)$  = cross spectral density,  $\phi_i, \theta_i = 1^{st}$  and  $2^{nd}$  random phase angle,  $x$  = longitudinal distance,  $N$  = number of sinusoidal components,  $\Delta n_i$  = bandwidth. Most of earlier research on bridge vehicle interaction used only unique roughness profile for both vehicle tracks and thus ignoring the rolling effect of vehicle. Two different road surface profile as show in **Fig. 4** is used for both tracks of vehicle to incorporate the bouncing, pitching and rolling effect.

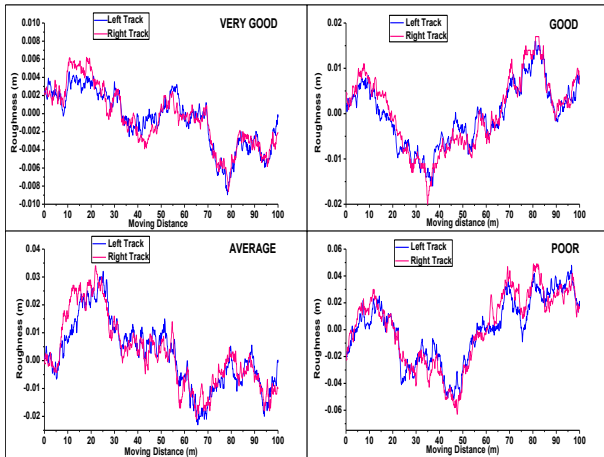


Fig. 4. Different road surface roughness profile

### 5 Dynamic Behaviors

Rayleigh damping, lumped mass system and 1% critical damping is assumed for 1<sup>st</sup> and 2<sup>nd</sup> mode of natural vibration. Newmark's  $\beta$  and Newton-Raphson methods are used to calculate structural response. To obtained vehicle initial condition, it is subjected to run 45m approach road having surface roughness same as that of bridge deck roughness before entering the bridge. The dynamic load effect measured in terms of deflection. The Dynamic Amplification Factor (DAF) is defined as shown in Eq. (3)

$$DAF (\%) = \left( \frac{R_{dyn} - R_{sta}}{R_{sta}} \right) * 100\% \dots (3)$$

Where  $R_{dyn}$  and  $R_{sta}$  are the absolute maximum dynamic and static response.

#### 5.1 Effect of loadings position

To obtain the maximum dynamic response of each girder, total 6 loadings position are considered as shown in Fig. 5 and in each case one track of vehicle is directly placed over the girder. Fig. 6 shows the effect of loading position on DAF is found under good roughness condition with vehicle speed 45 km/hr. Speed 45 km/hr is selected since it is responsible for highest DAF. From Fig. 6, it is found that the DAF of girders directly below the vehicle's wheel has similar value as defined by AASHTO (20%) and JRA (17.32%) formula. It is also clear that DAF of girder directly below the wheel has smaller value than that of others girder because of; girder directly below the wheel has highest static response than that of others. Hence all girders except girder 3 have about same DAF value under corresponding loading conditions. The girder 3 has more DAF value compared to others loading condition because of symmetric loading case 3 causing bending dominant vibration. Comparing to DAF of remote girder for each loading position, it is found that outer lane girder has higher value of DAFs compared to inner lane girder because of torsional vibration increase the dynamic response of outer lane girder.

#### 5.2 Effect of vehicle speed

Effect of vehicle speed on DAF studied for loading conditions 1, 3, & 6; vehicle speed from 15 to 120 km/hr with 15 interval and good roughness condition. Fig. 7 shows DAFs are extreme in lower (45km/hr) and upper speed limit (105 km/hr) and lowest at speed 75 & 90 km/hr. At 45 & 105 km/hr vehicle speeds, DAFs are highest because of high frequency dynamic response

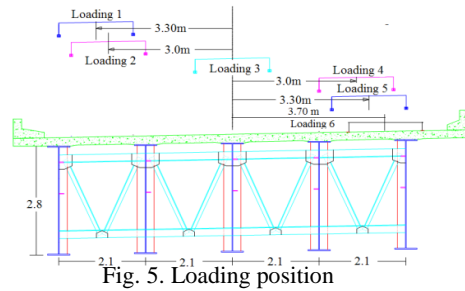


Fig. 5. Loading position

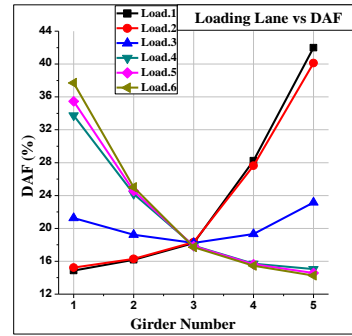


Fig. 6. Effect of loading positions DAF

caused by surface roughness. The acceleration PSD curve for speed 45 km/hr as shown in Fig. 8 indicates that, bridge 1<sup>st</sup> vertical vibration mode is coupled with pitching and bouncing mode of vehicle which leads to bridge resonance as well as high dynamic deflection. A reversal dynamic behavior is found under loading 1 & 6 and remote girder are found to be vibrate 2-3 times more compare with loaded girder because of torsional vibration. Again under loading 3, all girders are found to have same DAFs value.

#### 5.3 Effect of surface roughness

Fig. 9 represents the effect of surface roughness on DAF for loading conditions 1, 3, & 6 and vehicle speed 45 & 105 km/hr. A linear co-relation between roughness and DAF shows that worsen in roughness condition means higher value of DAF. Fig. 9 shows that obtain DAF value has good agreement with AASHTO and JRA formula under good roughness condition for central loading position whereas DAF value is overestimated others vehicle position. But for average and poor surface roughness condition, AASHTO and JRA formula fails to address the fact that impact factors is significantly under estimated. The loaded girder G3L3 is more critical compared to G1L1 & G6L6 because of significant static response exhibits for girder 1 & 5. Torsional vibration under loading 1 & 6 leads maximum differences in DAF value between loaded and remote girder but loading 3 reveals lower difference because of flexural dominant vibration. Fig. 10 derived under loading condition 6 reveals that AASHTO and JRA formula overestimated the DAF value (20 % and 17.32%) under very good and good roughness condition for heavily loaded girder for all velocity ranges. But for average and poor roughness condition, the DAF value is found much higher at lower and upper range of vehicle speed. The DAF value is always lowered than AASHTO and JRA specified value for speed 75km/hr for all roughness conditions because of low frequency dynamic response described as PSD plot in Fig. 10. The highest and 2<sup>nd</sup> highest DAF is found for 120 and 45 km/hr vehicle for speed for poor roughness condition.

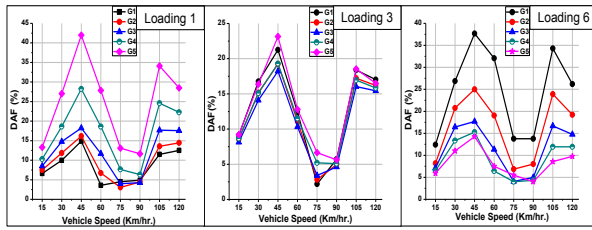


Fig. 7. Velocity effect on DAF

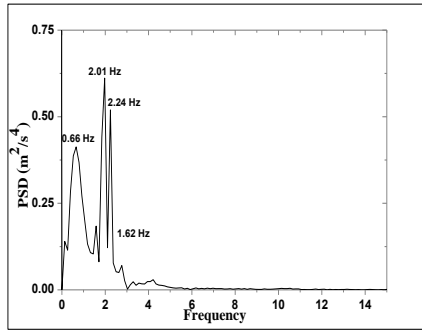


Fig. 8. PSD for 45 km/hr. of vehicle speed

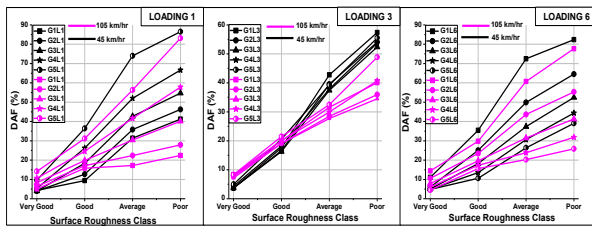


Fig. 9. Surface Roughness effect on DAF (loadings position)

**6 Conclusion**

Analytical study on dynamic amplification factors for horizontally curved multi-girder bridge has done using HS20-44 design truck. A fully computerized 3D bridge- vehicle coupled model has been developed using ANSYS program. From evaluation result followings conclusion can be drawn.

1. DAF of girders directly below vehicle’s wheel has a good agreement with value defined by AASHTO (20%) and JRA (17.32%) formula and of course these values are small compared to others girder’s value because of higher static response. Torsional vibration increases the dynamic response of outer lane girders yield higher value of DAF compared to inner lane girder.

2. The DAF fluctuates with vehicle speed and rougher the surface roughness means, higher value of DAF. For heavily loaded girder under poor surface roughness condition the DAF value reached to 1.70 and for remote girder is 2.25 for vehicle speed 120 km/hr. JRA formula is quite close to DAF value found under good roughness condition for lower and upper speed range but AASHTO formula always overestimated DAF value for good and very good surface roughness. For average and poor surface conditions both JRA and AASHTO formula under estimated the DAF value for upper and lower range of speed limit. At speed 75km/hr, DAF is lowest because of low frequency dynamic response of vehicle occurs due to surface roughness.

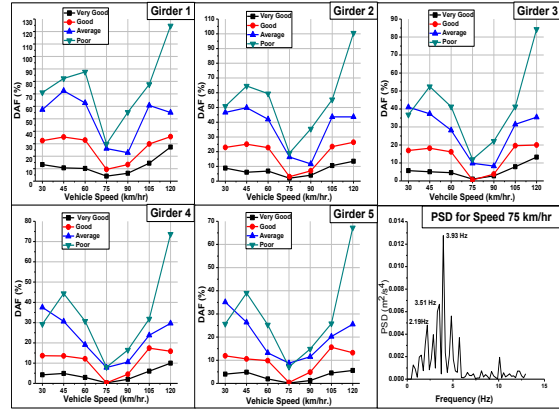


Fig.10. Surface Roughness effect on DAF for velocity

**References:**

- Sennah K. and Kennedy J. B.(1998): Vibrations of horizontally curved continuous composite cellular bridges, Canadian Journal of Civil Engineering, Vol.25, pp. 139-150.
- Senthilvasan J. : Thambiratan D.P; Brameld G.H. (2002): Dynamic response of a curved bridge under moving truck load. Engineering Structures 24, pp. 1283-1293.
- Sennah M.K., Zhang X., and Kennedy B. J (2004): Impact factors for horizontally curved composite box girder bridges. Journal of Bridge Engineering, Vol. 9, No. 6, pp. 512-520.
- Linzell D. G., Hall D., and White D. (2002): Historical perspective on horizontally curved I-girder bridge design in United States, Journal of Bridge Engineering, Vol. 9(3),pp. 1283-1293.
- Mermertas Vahit (1998): Dynamic interaction between the vehicle and simply supported curved bridge deck. Comput. Methods. Appl. Mech. Engg. 162, pp. 125-131.
- Huang D., Wang T. L. and Shahawy M. (1994): Dynamic behaviour of horizontally curved I-girder bridges. Computers & Structures Vol 57, No. 4. pp.703-714.
- Wang T. L., Li H., and Huang D (1992): Computer modeling analysis in bridge evaluation, Final report-Highway planning and research Program, Miami, Florida.
- Samaan M., Kennedy J. B. and Sennah K. (2007): Impact factors for curve continuous composite multiple-box girder bridges, Journal of Bridge Engineering, ASCE, Vol 12(1), pp. 80-88.
- Awall MR., Hayashikawa T., Matsumoto T., He X. (2012): Effects of bottom bracing on torsional dynamic characteristics of horizontally curved twin I-girder bridges with different curvatures. Earthq Eng and Eng Vib 11, pp. 149-162.
- Dodds C. J. and Robson J. D. (1973): The description of road surface roughness, Journal of Sound and Vibration, Vol 31(2), pp. 175-183.
- Honda H., Kajikawa Y. and Kobori T. (1982): Spectra of road surface roughness on bridges, Journal of the Structural Division, ASCE, Vol. 108 (ST9), pp. 1956-1966.
- Labarre R. P., Forbes R. T. and Andrew S. (1969): Measurement and analysis of road surface roughness, Motor Industry Research Association Report No. 1970.